Volume 17, Number 3, 2024. pp. 313-321

Jordan Journal of Physics

ARTICLE

# Structural and Luminescent Characteristics of Divalent Europium Activated Barium Aluminate with the Tridymite Structure Synthesized by the Sol-Gel Technique

**Ruba I. Alzubi**[a,b], **Yazan A. Mousa**[b] and **Hassan K. Juwhari**[a]

[a] *Department of Physics, School of Science, University of Jordan, Amman 11942, Jordan.*
[b] *Jordan Atomic Energy Commission, Amman 11934, Jordan.*

***Doi:*** **https://doi.org/10.47011/17.3.6**
*Received on: 07/08/2022;* *Accepted on: 27/11/2022*

**Abstract:** In this study, alkaline earth aluminates were investigated as potential hosts for new blue luminescent materials with nanoparticles. $Ba_{1-x}Eu_xAl_2O_4$ with the stuffed tridymite hexagonal structure was successfully synthesized at 900 °C under controlled sol-gel conditions. Divalent europium was effectively used to activate this host material, producing a brilliant blue-emitting phosphor. Its spectral photoluminescence at 408 nm appears to be in a region close to the laser blue region, with chromaticity coordinate values suitable for the standard blue of the PAL TV system.

**Keywords:** Blue phosphors, $BaAl_2O_4$, Divalent Europium ($Eu^{2+}$), Sol-Gel synthesis, Critical energy transfer.

## Introduction

New phosphors are in constant demand, mostly for flat panel display applications where specific color rendition and adequate chemical and physical stability are required under the harsh environment of display operations [1-3]. Potential new blue phosphors are of great interest, especially if their optimal emission peaks are close to 405 nm.

The most common alkaline earth aluminate $MAl_2O_4$ ($M$ = *Ba*, *Ca*, and *Sr*) is the $BaAl_2O_4$ hexagonal structure (space group $P6_322$, 182). Various synthesis methods have been used to prepare $BaAl_2O_4$. These include solid-state reactions [4, 5], combustion [6, 7], and sol-gel synthesis [8]. When these techniques are compared to each other, the sol-gel technique offers several advantages, including relatively low preparation temperatures, ease of stoichiometry control, and the no need for expensive setups or equipment.

Divalent europium $Eu^{2+}$ is one of the most common rare-earth elements used for doping $BaAl_2O_4$ among alkali metal-based aluminate phosphors [8-10]. Consequently, considerable efforts have been dedicated to studying the reduction processes of $Eu^{3+}$ to $Eu^{2+}$ during phosphor preparation [11-13]. These techniques usually require complicated systems of furnaces coupled to quartz tubes through which inert gases are forced to flow to produce reducing atmospheres. These reducing atmospheres may include only $H_2$ or a mixture of gases such as $N_2$ + $H_2$ [14]. Alternatively, a carbon atmosphere can be employed as a simplified method, sometimes favored for its ease of application across various systems [2]. Moreover, based on the model of the charge compensation mechanism, some complexes tend to allow spontaneous self-reduction of their constituents in air [15].

**Corresponding Author:** Hassan K. Juwhari **Email**: h.juwhari@ju.edu.jo

The current work presents findings on the barium aluminate $BaAl_2O_4$ which can be activated with divalent europium to yield blue photoluminescence. Previous work on $BaAl_2O_4$ produced luminescence around 500 nm due to the effect of the preparation methods and conditions [9].

## Experimental Methods

In a modified sol-gel technique, powder samples of $Ba_{1-x}Eu_xAlO_4$ with varying concentrations of 0-8 mole % were prepared. The starting materials were powders of $Al(NO_3)_3.9H_2O$ (98% extra pure, Alpha Chemika), $Ba(NO_3)_2$ (ACS: > 99.0% KT, Puriss. P.A.), and citric acid anhydrous ($C_6H_8O_7{\cdot}H_2O$, extra pure). $Eu(NO_3)_3.5H_2O$ (99.9% trace metals basis, ALORICH) was added as the activator. Barium nitrate and aluminum nitrate were used as the source for metals, while citric acid acted as a polymerizing and chelating agent. The stoichiometric amount of citric acid was added to the solution in a 1:1 molar ratio with respect to the total cations ($Ba^{2+}$ and $Al^{3+}$) to complex the cations. All the starting materials were made part of a homogeneous solution in deionized water, D.I. [10]. The resultant clear solution was then heated for 30 minutes on a magnetic stirrer. Meanwhile, an ethylene diamine was added to this clear solution drop by drop to adjust the pH to 6. The mixture was then dried overnight using an infrared lamp.

The collected mixture was then placed in a muffle furnace at 700 °C for 6 hours to remove all organic components. The recovered powder was later divided into two equal batches, each transferred to a separate crucible. These crucibles were placed individually in a regular muffle furnace and heated at 900 °C for 3 hours with a heating rate of 5 °C/min. One crucible was annealed in the presence of air, while the other was treated in a carbon atmosphere using a double crucible technique. In this technique, the sample is placed in the inner crucible, while activated charcoal powder fills the space between the inner and outer crucibles.

## Results and Discussion

$BaAl_2O_4$ was prepared in both pure and doped phases, as shown in Figs. 1 and 2, and was found to be stable up to at least 1100 °C. The X-ray diffraction patterns agreed well with the reference pattern from the International Collection of Diffraction Data for Powders (ICDD Card No. 96-100-8090). These figures show several doping concentrations of $Eu^{2+}$ synthesized in air (1-8 mole %) and in a carbon atmosphere (1-3 mole %) compared to the ICDD standard card for $BaAl_2O_4$.

The calculated unit cell parameters for the non-doped pure phase were a = b = 5.152 Å and c = 8.744 Å. These results can be compared compared to the values of Ref. [18], where a = b = 5.209 Å and c = 8.761 Å. These results were based on the collected diffraction pattern. Moreover, utilizing the Debye-Scherer's equation for the calculation of the average crystallite sizes at the maximum peak (h k l) = (0 1 2) for the hexagonal configuration, yielded values ranging from ~32 to 40, nm depending on the calcination time and duration. XRD measurements were performed using a Shimadzu XRD-7000 diffractometer with Cu $K_\alpha$ radiation ($\lambda$ = 1.5404 Å).

The particle size of freshly prepared powder samples was studied utilizing scanning electron microscopy (SEM, JEOL JSM6300 model). The images in Fig. 3 show a moderately well-controlled distribution of particle sizes, with the nanocrystalline nature of the samples apparent. Moreover, the samples prepared in the presence of activated charcoal, as shown in Fig. 3(b), exhibited a larger density of relatively tiny particles residing on top of larger grains compared to samples prepared in air, as depicted in Fig. 3(a).

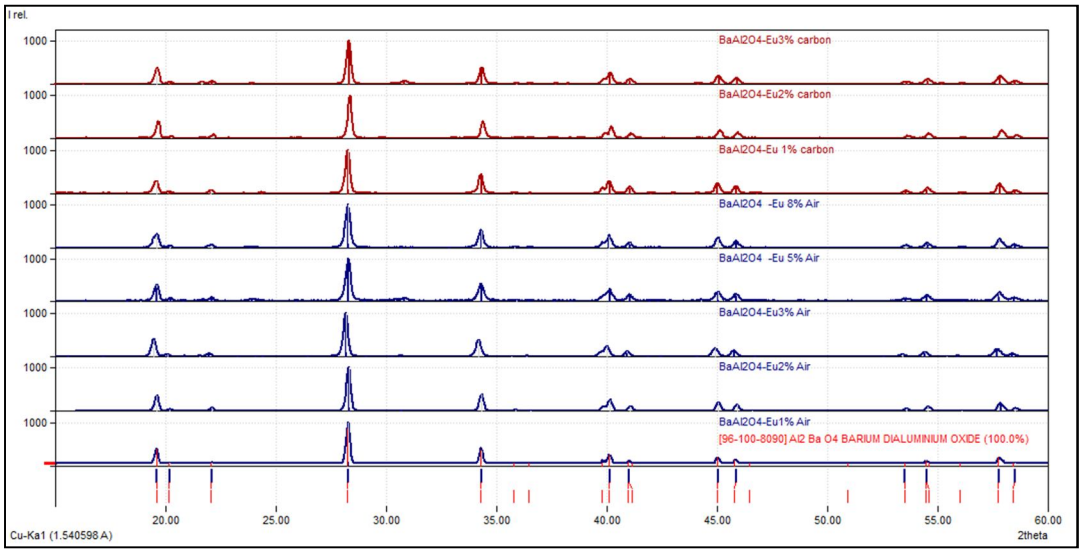


FIG. 1. Powder XRD of sol-gel synthesized $BaAl_2O_4$ annealed at 900°C for 3 h, with various concentrations of $Eu^{2+}$, both in air and in the presence of activated charcoal.

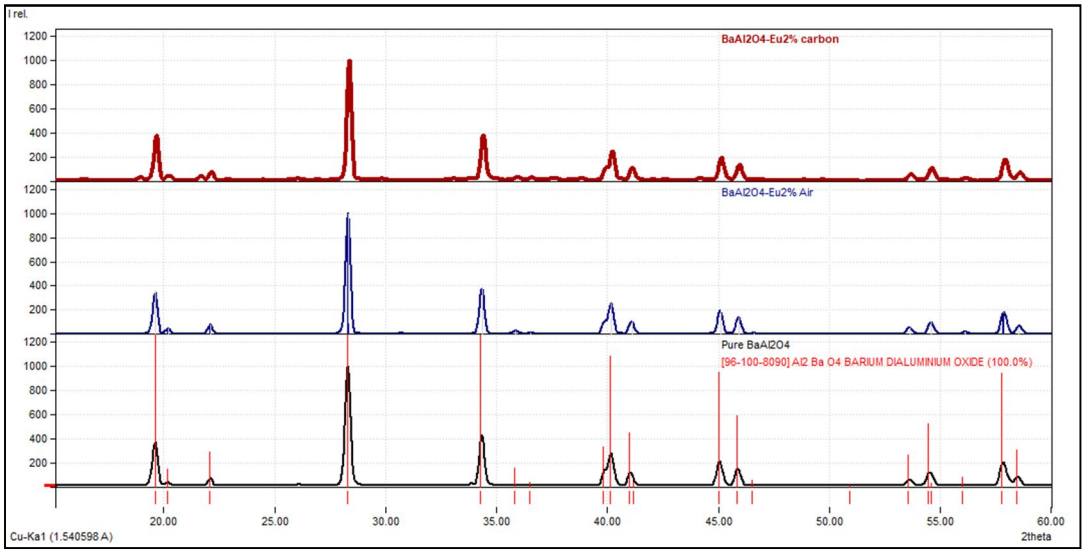


FIG. 2. Enlarged view of powder XRD for sol-gel synthesized $BaAl_2O_4$ annealed at 900 °*C* for 3 h (pure phase vs. 2 mole % $Eu^{2+}$, annealed in air and in the presence of activated charcoal), compared to ICDD standard card No. 96-100-8090.

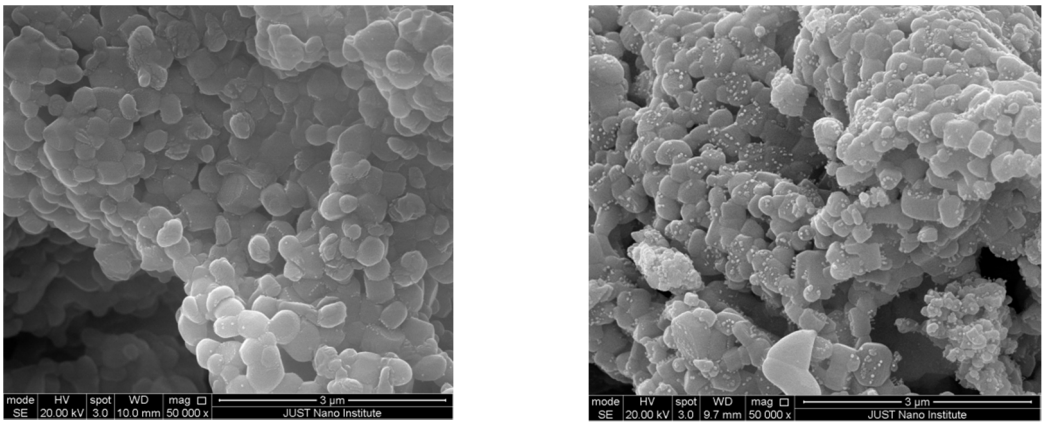


(a) (b)

FIG. 3. SEM images of the freshly prepared $Ba_{0.99}Eu_{0.01}AlO_4$ in (a) air and (b) the presence of activated charcoal. Note the higher density of smaller particles atop the larger ones in the sample prepared in the presence of carbon atmosphere compared to the sample prepared in air.

The room temperature photoluminescent spectra (PL) of the freshly prepared powders were recorded using a Cary Eclipse (Varian) spectrofluorometer. The instrument settings included adjusting the voltage to 600 V to maximize the output of the Xenon lamp, which served as the light source. The excitation spectra were scanned and collected at a photoemission wavelength of 495 nm for both samples prepared in air and under a carbon atmosphere. The emission spectra were scanned at excitation wavelengths of 334 and 325 nm for samples prepared in air and under a carbon atmosphere, respectively. The emission spectra of $Ba_{1-x}Eu_xAlO_4$ prepared in air, shown in Fig. 4(a), reveal two spectral broa-band emissions peaking at ~ 405 and 495 nm. Similar dual emission peaks have been reported recently [16], attributed to two distinct sites available for rare earth cations in the $BaAl_2O_4$ tridymite structure at the Ba Sites [19, 20]. These different sites likely favor different environmental preparation conditions. This was obvious from the distinct luminescent behaviors of the two samples shown in Figs. 4(a) and 4(b), prepared in air and under a carbon atmosphere, respectively.

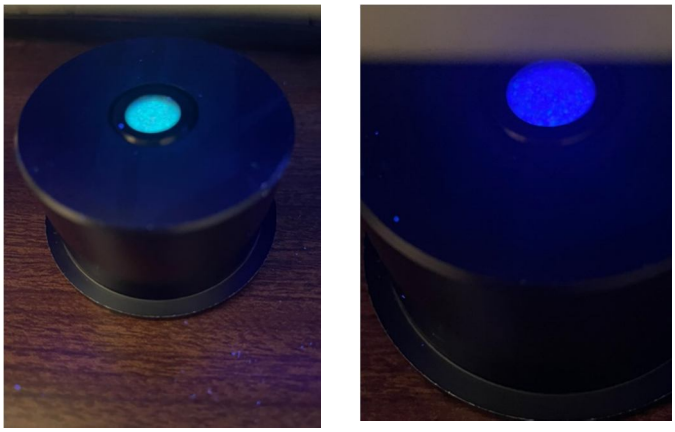

(a) in air (b) in carbon

FIG. 4. Emission behavior of the two samples of $Ba_{0.98}Eu_{0.02}AlO_4$ prepared in (a) air and (b) under the influence of carbon. Both samples were excited with a UV xenon handheld lamp at 365 nm.

Usually, photoluminescence and absorption spectra of divalent europium exhibit broad bands due to electronic transitions from the ground state $^8S_{7/2}$ ($4f^7$) to the crystal field components of the $4f^65d$ excited state configuration [21]. This emission of the $Eu^{2+}$ can occur at any wavelength, extending from the blue region to the red region of the visible light, depending on the host material structure and the preparation conditions. The reduction of $Eu^{3+}$ to $Eu^{2+}$ in solid-state compounds prepared at high temperatures in air is generally governed by four conditions (model of charge compensation mechanism): (1) the host compounds must not contain any oxidizing ions; (2) the cation (europium in this investigation) must substitute a divalent cation in the host matrix; (3) the substituted cation must have a radius of the order comparable to that of the substituent ($Eu^{2+}$) ion; and (4) the host compound should possess an appropriate structure, typically involving tetrahedral anion groups $BO_4$, $SO_4$, $PO_4$, $SiO_4$ or $AlO_4$. Even though all these conditions may apply to the studied host structure, the varying luminescence intensities with different dopant concentrations suggest that spontaneous reduction of $Eu^{3+}$ to $Eu^{2+}$ can't be a complete process without a reducing atmosphere. Citric acid used in the preparation may indeed act as a reducing agent, but this reduction was limited. Applying a reducing atmosphere results in further reduction and apparently to higher concentrations of $Eu^{2+}$ cations. Considering this is the case, then the more reduced the dopants, the more help in producing the luminescence is recorded and shown in the figures.

As shown in Fig. 5(a), the photoluminescence spectra of $Ba_{1-x}Eu_xAlO_4$ (x = 0.01, 0.02, 0.03, 0.05, and 0.08) powders synthesized in air, in the wavelength range of 400 to 600 nm, reveal two broad peaks centered around 415 and 495 nm. The 495 nm band is more pronounced than the other band at the lower wavelength when samples are heated in air. We were successful in forcing luminescence to be concentrated near the wavelength of 408 nm at the expense of the other emission band by adjusting the sintering atmosphere to include carbon during this process and controlling the heating rate at a relatively slow 5°C/min up to soaking temperature. This

treatment resulted in the photoluminescence shown in Fig. 5(b) for $BaAl_2O_4$ doped with $xEu^{2+}$ (x = 0.01, 0.02, 0.03, 0.05, and 0.08), where the rare-earth europium divalent cations favor residing on one of the barium sites. Moreover, the presence of carbon during the heating of the samples enhanced the relative luminescence intensity, as shown in Fig. 5(c).

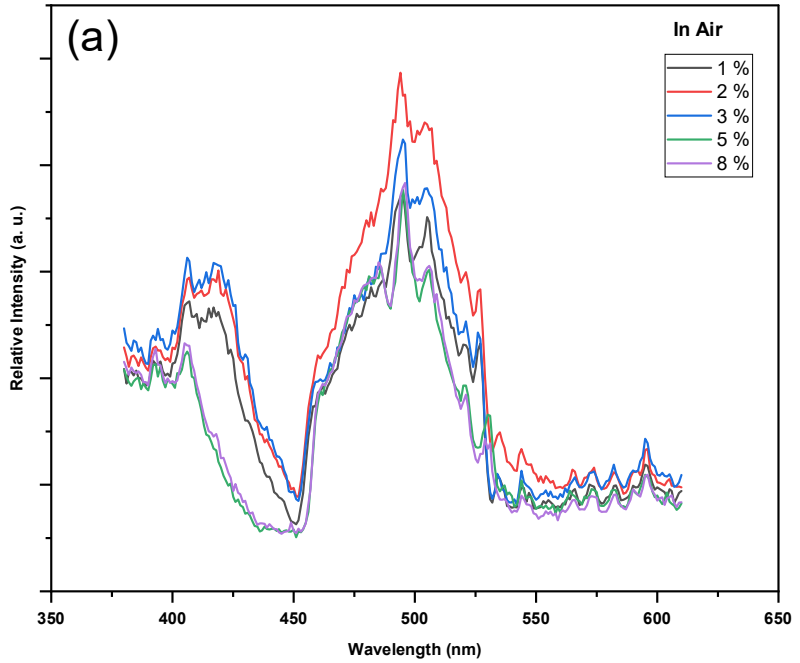


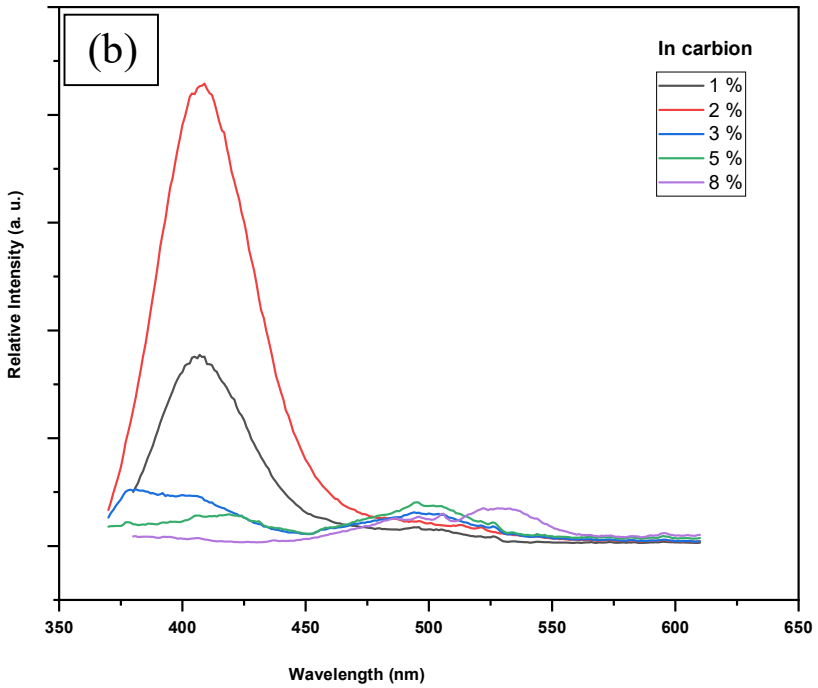

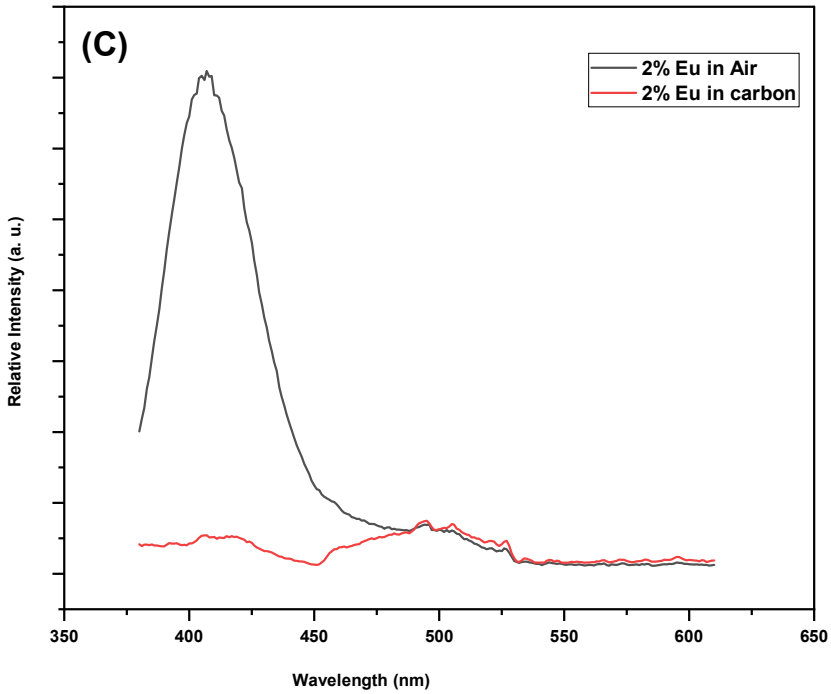


FIG. 5. Emission spectra of $Ba_{1-x}Eu_xAlO_4$. The spectral bandpasses were kept at 2.5 nm for both the excitation and emission monochromators for all samples for comparison reasons. Samples were prepared (a) in air and (b) in the presence of carbon. (c) Comparison of spectra.

In an attempt to estimate the critical energy-transfer distance ($r_c$) for divalent europium activators in the host matrix material, we utilized the subsequent equation [15]: $R_c = 2[3V/4\pi X_c Z]^{1/3}$. Here, $Z = 2$ represents the available cation sites within the unit cell acknowledging two accessible distinct crystallographic sites for divalent europium in the $BaAl_2O_4$ crystal structure. $X_c$ represents the $Eu^{2+}$ critical concentration in the $BaAl_2O_4$ host material (~ 0.02) and $V$ = 198.69 Å$^3$ represents the unit cell volume. As such, the $Eu^{2+}$ critical energy-transfer distance was approximated to be 21.2 Å.

Three competing mechanisms could describe the non-radiative processes between $Eu^{2+}$ activators: excitation–emission spectral overlap, exchange-intercalation, and electric-multipolar intercalation. Out of these, the transfer-intercalation necessitates shorter critical distances of a few Å or less, separating the donor-acceptor pairs, as it is typically responsible for the forbidden energy-transfer transitions. However, since the electric dipole ($^8S_{7/2} \rightarrow 5d$) transition of the divalent europium is parity-allowed [22], the exchange-intercalation mechanism can be neglected in $BaAl_2O_4:Eu^{2+}$ phosphors. Moreover, the registered insignificant spectral overlap in the $BaAl_2O_4:Eu^{2+}$ phosphors (Fig. 5) suggests that the radiation-reabsorption mechanism is to be disregarded also for this particular luminescent behavior since this mechanism can only be considered when substantial overlap is shown between the excitation and emission spectra. Hence, we are only left with the possibility that the electric-multipolar intercalation processes of divalent europium activators in $BaAl_2O_4$ are possibly accountable for the photoluminescence quenching and the energy transfer.

The blue emission near 408 nm of the $BaAl_2O_4:0.02Eu^{2+}$, along with its excitation spectrum shown in Fig. 6, indicates that this material could be a promising candidate for blue phosphors. This potential makes it worthwhile to check its chromaticity coordinates for comparison with other emerging blue phosphors.

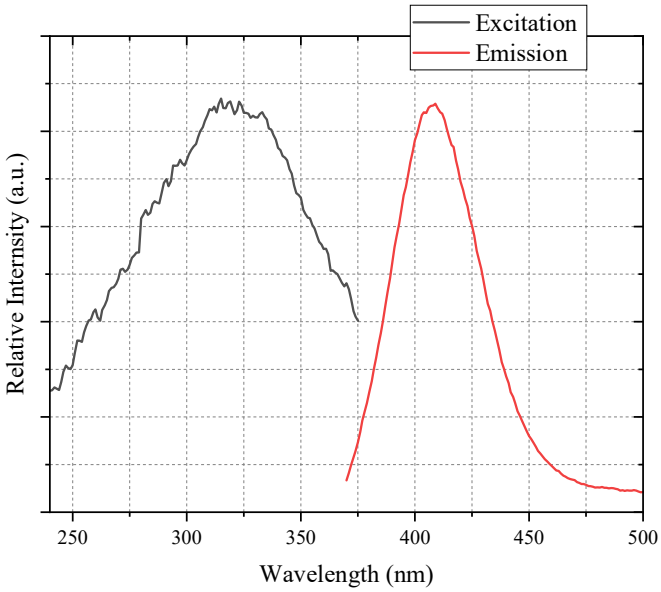


FIG. 6. Excitation and emission spectra for $Ba_{0.98}Eu_{0.02}Al_2O_4$. The spectral monochromator slits were set to 2.5 nm, with medium voltage setting adjusted to 600 V.

The chromaticity coordinates of the sol-gel prepared $BaAl_2O_8:Eu^{2+}$ powder samples based on the CIE 1931 were calculated depending on the emission spectra and plotted on the chromaticity diagram (Fig. 7). It is worth mentioning here that the white-point chromaticity coordinates are (0.333, 0.333). In order to display the degree of the color purity of the luminescent emission, one typically determines how far the color is shifted from the saturated color locus at the spectralboundary. Hence, color purity is calculated as the length of the line representing how far the calculated chromaticity coordinates with respect to the chromaticity coordinates of the white point divided by the length of the line representing how far the chromaticity coordinates of the saturated color locus compared to the chromaticity coordinates of the white point multiplied by 100%. Based on this procedure, it is found that the $BaAl_2O_8:Eu^{2+}$ color purity amounts to 88.4%, compared to 94.9% reported for $CaB_2Si_2O_8:Eu^{2+}$ which was found suitable for the NTSC values for the blue standard [22], and 83.9% for the Osram-Sylvania BAM (used as a reference for blue phosphor) [23].

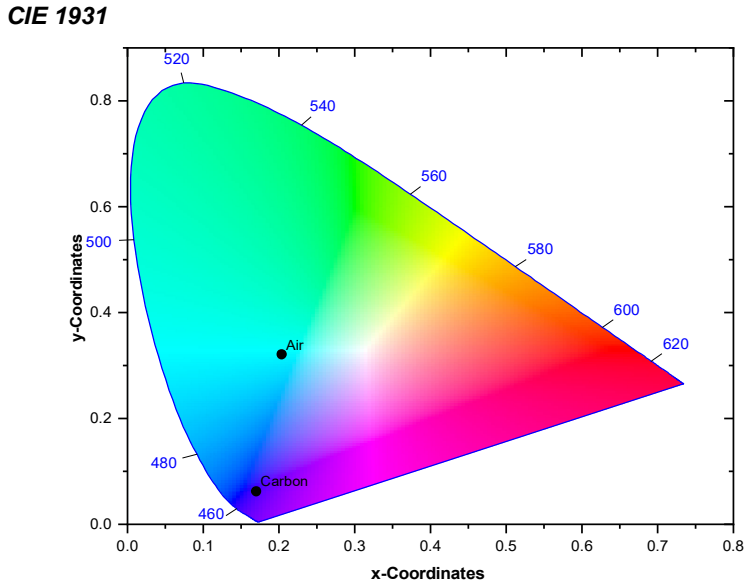


FIG. 7. CIE 1931 chromaticity diagram with chromaticity coordinate points labeled “Carbon” and “Air”, indicating the calculated color coordinates obtained from the luminescence emission spectra of sol-gel prepared $Ba_{1-x}Al_2O_4:xEu^{2+}$ phosphor samples either in air or in the presence of carbon.

The two points for the 2% doped samples prepared in air and under a reducing atmosphere are placed on the chromaticity diagram adjacent to the saturated color locus and specified on the color space diagram by their locations. The color purity coordinates of the $Ba_{0.98}Eu_{0.02}Al_2O_4$ powder sample prepared with activated charcoal are listed in Table 1, alongside those of $Ca_{0.96}Eu_{0.04}B_2Si_2O_8$ and the Osram Sylvania Blue reference phosphor. Moreover, the color purity of the prepared $Ba_{0.98}Eu_{0.02}Al_2O_4$ powder sample, shown in Fig. 7, is found to be close to the standard CIE PAL TV primary values for blue [23].

TABLE 1. CIE chromaticity coordinates of sol-gel synthesized barium aluminate activated with divalent europium in the presence of carbon, compared to divalent europium-activated danburite and the BAM Osram Sylvania blue reference phosphor type 2461.

| Concentration (mol %) | X Coordinate | Y Coordinate | |
|---|---|---|---|
| $Ba_{0.98}Eu_{0.02}AlO_4$ | 0.1697 | 0.0630 | This Work |
| $Ca_{0.96}Eu_{0.04}B_2Si_2O_8$ | 0.1427 | 0.0576 | Synthetic Danburite [22] |
| *BAM* Reference | 0.1417 | 0.1072 | [Osram-Sylvania type 2461 Reference phosphor] |

## Conclusion

Phase-pure nanocrystalline barium aluminate with the stuffed tridymite structure was successfully prepared via a modified sol-gel reaction of barium nitrate and aluminum nitrate. When activated by $Eu^{2+}$, it exhibited initial emission from cations residing on both $Ba^{2+}$ competing sites. Annealing under a reducing atmosphere resulted in an enhanced probability of reducing $Eu^{3+}$ and hence improving their likelihood of occupying favorable sites. This process resulted in a brilliant, single blue broad-band phosphor with a maximum centered at ~ 408 nm. This wavelength, suitable for the laser blue color rendition, is produced at the optimal doping concentration of about 2 mol.% of $Eu^{2+}$ in the $BaAl_2O_4$ host. In addition, the critical energy transfer distance was calculated to be ~ 21.2 Å. The calculated chromaticity coordinates of these successfully sol-gel synthesized phosphors were found to be (0.169, 0.063). Finally, based on the 1931 CIE chromaticity diagram and the tables of the PAL TV systems for blue phosphors, these prepared materials appear to be promising candidates.

## Acknowledgment

This work was partially accomplished during the sabbatical year of one of the authors (H. K. Juwhari) spent at the University of Jordan during the academic year 2019/2020. This research is also partially funded by the School of Graduate Studies at the University of Jordan (R. I. Al-Zubi and H. K. Juwhari).

## References

[1] Singh, D., Tanwar, V., Simantilleke, A.P., Mari, B., Kadyan, P.S., and Singh, I., J. Mater. Sci.: Mat. Elect., 27 (3) (2016) 2260.

[2] Guzmán-Rocha, M., Oliva, J., Diaz-Torres, L.A., and Montes, J., Solgel. Sci. Technol., 95 (2) (2020) 423.

[3] Mothudi, B.M., Ntwaeaborwa, O.M., Botha, J.R., and Swart, H.C., Physica B Condens Matter., 404(22) (2009) 4440.

[4] Sathaporn, T. and Niyomwas, S., Energy Procedia., 9 (2011) 410.

[5] Peng, M. ad Hong, G., J. Lumin., 127 (2) (2007) 735.

[6] Satapathy, K.K., Mishra, G.C., and Khan, F., Chem. Sci. Trans., 2 (2013) 1262.

[7] den Engelsen, D., Fern, G.R., Ireland, T.G., Yang, F., and Silver, J., J. Opt. Mater. Express, 10 (8) (2020) 1962.

[8] Maphiri, V.M., Mhlongo, M.R., Hlatshwayo, T.T., Motaung, T.E., Koao, L.F., and Motloung, S.V., Opt. Mater., 109 (2020) 110244.

[9] Araujo, R.M., dos Santos Mattos, E.F., dos Santos Júnior, B.F., Rezende, M.V.D.S., Valerio, M.E., and Jackson, R.A., J. Lumin., 236 (2021) 118011.

[10] Lephoto, M.A., Ntwaeaborwa, O.M., Pitale, S.S., Swart, H.C., Botha, J.R., and Mothudi, B.M., Physica B Condens Matter, 407 (10) (2012) 1603.

[11] Bierwagen, J., Delgado, T., Jiranek, G., Yoon, S., Gartmann, N., Walfort, B., and Hagemann, H., J. Lumin., 222, (2020) 117113.

[12] Xu, Y., Sun, Z., Wei, Y., Jia, M., Hou, B., Li, X., and Fu, Z., J. Am. Ceram. Soc., 103 (10) (2020) 5721.

[13] Xie, H., Lu, J., Guan, Y., Huang, Y., Wei, D., and Seo, H.J., Inorg. Chem., 53 (2) (2014) 827.

[14] Aitasalo, T., Hölsä, J., Jungner, H., Lastusaari, M., and Niittykoski, J., J. Phys. Chem. B, 110 (10) (2006) 4589.

[15] Wang, Z., Liu, Y., Chen, J., Fang, M., Huang, Z., and Mei, L., J. Adv. Ceram., 6 (2) (2017) 81.

[16] Rodrigues, L.C.V., Stefani, R., Brito, H.F., Felinto, M.C.F.C., Hölsä, J., Lastusaari, M., Laamanen, T., and Malkamäki, M., J. Solid State Chem., 183 (10) (2010) 2365.

[17] Mishenina, L.N., Selyunina, L.A., and Botvina, T. M., Key Eng. Mater., 670 (2016) 95.

[18] Hörkner, W. and Müller-Buschbaum, H.Z., Anorg. Allg. Chem., 451 (1) (1979) 40.

[19] Volhard, M., Yu, L., den Engelsen, D., Fern, G.R., Ireland, T.G., and Silver, J., Opt. Mater. Express, 10 (8) (2020) 1951.

[20] Stefani, R., Rodrigues, L.C.V., Carvalho, C.A.A.D., Felinto, M.C.F.D.C., Brito, H.F.D., Lastusaari, M., and Hölsä, Opt. Mater. Amst., 31 (12) (2009) 1815.

[21] Marí, B., Singh, K.C., Verma, N., Mollar, M., and Jindal, Trans. Indian Ceram. Soc., 74 (3) (2015) 157.

[22] Juwhari, H.K. and White, W.B., Mater. Lett., 88 (2012) 16.

[23] Broadbent, A.D., Color Res. Appl., 29 (4) (2004) 267.